TISSUE ENGINEERING: Part C
Volume 23, Number 10, 2017

DOI: 10.1089/ten.tec.2017.0307

termis
Tissue Engineering
& Regenerative Medicine
International Society

METHODS ARTICLE

PCL-PDMS-PCL Copolymer-Based Microspheres Mediate Cardiovascular Differentiation from Embryonic Stem Cells

Liqing Song, MS,[1] Mohammad Faisel Ahmed, BS,[2] Yan Li, PhD,[2,3] Julie Bejoy, MS,[1] Changchun Zeng, PhD,[2,3] and Yan Li, PhD[1]

Poly-ε-caprolactone (PCL) based microspheres have received much attention as drug or growth factor delivery carriers and tissue engineering scaffolds due to their biocompatibility, biodegradability, and tunable biophysical properties. In addition, PCL and polydimethylsiloxane (PDMS) can be fabricated into thermoresponsive shape memory polymers for various biomedical applications (e.g., smart sutures and vascular stents). However, the influence of biophysical properties of PCL-PDMS based microspheres on stem cell lineage commitment has not been well understood. In this study, PDMS was used as soft segments of varying length to tailor the elastic modulus of PCL-based copolymers. It was found that lower elastic modulus (<10 kPa) of the tri-block copolymer PCL-PDMS-PCL promoted vascular differentiation of embryonic stem cells, but the range of 60–100 MPa PCL-PDMS-PCL had little influence on cardiovascular differentiation. Then different sizes (30–140 μm) of PCL-PDMS-PCL microspheres were fabricated and incorporated with embryoid bodies (EBs). Differential expression of KDR, CD31, and VE-cadherin was observed for the EBs containing microspheres of different sizes. Higher expression of KDR was observed for the condition with small size of microspheres (32 μm), while higher CD31 and VE-cadherin expression was observed for the group of medium size of microspheres (94 μm). Little difference in cardiac marker α-actinin was observed for different microspheres. This study indicates that the biophysical properties of PCL-PDMS-PCL microspheres impact vascular lineage commitment and have implications for drug delivery and tissue engineering.

Keywords: poly-ε-caprolactone, copolymers, embryonic stem cells, cardiovascular differentiation, microspheres

Introduction

Cardiovascular disease is the leading cause of death in the world and accounts for more than one-third of all deaths in the United States each year.[1] The total direct and indirect cost of cardiovascular disease and stroke is estimated to be $315 billion in 2010 in the United States.[1] The treatments of cardiovascular diseases require efficient systems to generate sufficient cardiovascular cells, tissues, and models for the development of vascular prosthetics, new drugs, or the disease-relevant models.[2,3] Pluripotent stem cells (PSCs), including embryonic stem cells (ESCs) and induced PSCs (iPSCs), are ideal cell sources to generate unlimited numbers of cardiovascular cells or to construct cardiovascular tissues for cell therapy, drug screening, and disease modeling.[4–9]

Efficient scalable differentiation of cardiovascular cells from PSCs usually relies on the microspheres/microparticles to support cell adhesion or to deliver the inducing growth factors in suspension.[10–12] Microspheres of different materials such as gelatin, agarose, and poly lactic-co-glycolic acid (PLGA) were shown to induce differential expression of genes and proteins for mesoderm and endoderm lineage commitment from PSCs.[13] In addition, the biophysical properties (e.g., microsphere size and the elastic modulus) of microspheres have profound effects on stem cell lineage commitment. For example, the comparison of different particle sizes showed the accelerated differentiation and more cystic embryoid bodies (EBs) when delivering retinoic acid using small size particles (1–11 μm).[14] PLGA microparticles were also studied in the range of 100–240 μm during chondrogenic differentiation of mesenchymal stem cells (MSCs), where the use of particles of 175 μm resulted in

Departments of [1]Chemical and Biomedical Engineering and [2]Industrial and Manufacturing Engineering, FAMU-FSU College of Engineering, Florida State University, Tallahassee, Florida.
[3]High-Performance Materials Institute (HPMI), Florida State University, Tallahassee, Florida.
The preliminary results of this study were presented in 2015 Annual Meeting of American Institute of Chemical Engineers (AIChE), Salt Lake City, Utah, November 8–13, 2015.

the cartilage-like matrix formation (i.e., collagens I and II and glycosaminoglycan).[15] PLGA microspheres were incorporated into the collagen gels to increase the stiffness of extracellular microenvironment and promoted osteogenic differentiation of MSCs by providing stiff microenvironment.[16] All these studies indicate that biophysical properties of microspheres or microparticles influence stem cell differentiation.

Poly-ε-caprolactone (PCL) based microspheres have wide applications in drug delivery and tissue engineering applications.[17,18] PCL is biocompatible with a variety of human tissues and its long-term biodegradability allows the drug release up to several months.[19] In addition, PCL-based materials have flexible mechanical properties (Young's modulus, tensile strength, etc.) by tailoring their structures.[18] PCL-based microspheres (about 30–210 μm) can be fabricated by various methods such as emulsion solvent evaporation, spray drying, solution enhanced dispersion, and so on.[17,18] Moreover, PCL allows the modification of physical, chemical, and mechanical properties through the formation of copolymers, for example, gelatin, chitosan, polydimethylsiloxane (PDMS), poly(ethylene glycol), poly(vinyl alcohol), and PLGA, or forming composites by blending with other polymers.[18]

Among different PCL-based materials, the copolymers of PCL-PDMS-PCL have unique properties and can be used to synthesize and fabricate thermoresponsive shape memory polymer (SMP) based materials.[20,21] SMPs have been used in biomedical devices, such as smart sutures, vascular stents, and tissue engineering scaffolds.[22] For example, the cell alignment (i.e., cytoskeleton orientation and nuclear alignment) of MSCs was shown to be modulated by the shape memory-actuated fiber alignment of the scaffolds.[23] In particular, PDMS can serve as soft segments of varying length to tailor the mechanical properties of PCL (serving as hard segments)-based polymers. Varying the segment lengths of PCL and PDMS can tune the mechanical properties of the resulting copolymers to fabricate the copolymers with desired stiffness.[20]

The objective of the present study is to fabricate PCL-PDMS-PCL microspheres and evaluate the influence of biophysical properties (i.e., microsphere size and elastic modulus) of PCL-PDMS-PCL copolymers on cardiovascular differentiation of ESCs. This study indicates the importance of biophysical properties of microspheres on cardiovascular lineage commitment and has the significance in biomaterial design for stem cell-based tissue engineering, cellular differentiation, and growth factor delivery.[24]

Materials and Methods

Materials

ε-caprolactone monomer, poly (dimethylsiloxane)-bis (3-aminopropyl) terminated (molecular weight [Mn] ~2500 g/mol), hexamethylene diisocyanate (HDI), stannous 2-ethylhexanoate, and solvents were purchased from Sigma-Aldrich (St. Louis, MI). Aminopropyl terminated polydimethylsiloxane DMS A12 (Mn ~1000 g/mol), DMS A15 (Mn ~3000 g/mol), DMS A21 (Mn ~5000 g/mol), and DMS A31 (Mn ~25,000 g/mol) were purchased from Gelest, Inc. (Morrisville, PA).

Synthesis of PCL-PDMS-PCL copolymers

Macromers of PCL_n-block-$PDMS_m$-block-PCL_n were synthesized by ring-opening polymerization of ε-caprolactone in the presence of $NH_2 - PDMS_m - NH_2$ and tin-catalyst (Fig. 1A).[20,25] The repeat units of PCL segment length were varied at $n = 20$, 40, and 50. The PDMS segment lengths were varied at $m = 10$, 34, 58, and 296. Specifically, various amounts of ε-caprolactone (37.75, 75.49, or 94.36 mmol), aminopropyl terminated polydimethylsiloxane DMS A12, A15, A21, or A31 (2.20 mmol), and stannous 2-ethylhexanoate (0.123 mmol) were added into a 250 mL three-neck flask at 145°C and stirred for 24 h when the copolymers were synthesized. Copolymers with $PDMS_{28}$ were synthesized with poly (dimethylsiloxane)-bis(3-aminopropyl) terminated similarly.

For the chain propagation between oligomers by adding HDI as a coupling agent (Fig. 1B), the synthesized oligomers were transferred into a 1000 mL flask and cooled down from 145°C to 100°C. Synthesized oligomers were dissolved in 1,2-dichloromethane and water. The 1,2-dichloroethane was then removed at 100°C until no bubbles existed in the solution. When the flask was cooled down from 100°C to 50°C, two drops of stannous octanoate and 0.002 mole HDI were added into the system sequentially and reacted for 5 h.

Dynamic mechanical analysis

Dynamic mechanical analysis (DMA) was used to measure the Young's modulus of different copolymers. The samples were characterized using dynamic mechanical analyzer (Q800; TA Instruments). For tensile modulus, the rectangular samples were exerted under strain at a strain rate of 0.1 min^{-1} and 30°C. Compressive modulus was measured for samples (low elastic modulus) that cannot be measured for tensile modulus. In a compression model, the cylindrical samples were compressed with a 15-mm compression clamp at a strain rate of 0.1 min^{-1} and 30°C. The Young's modulus was calculated based on the initial slope of the stress–strain curve.

Differential scanning calorimetry analysis and ^{1}H-NMR

For differential scanning calorimetry (DSC) analysis, the samples were run on the differential scanning calorimeter (Q100; TA Instruments) from 30°C to 100°C at a heating rate of 10°C/min. The samples were then cooled down from 100°C to 30°C at a cooling rate of 10°C/min. The melting point Tm was calculated from the heat flow-temperature curve. The enthalpy change was determined from the endothermic melting peak. The % crystallinity was calculated using the equation:

$$\%\ crystallinity = \frac{\Delta H_m}{\Delta H_m^0} \times 100$$

where ΔH_m is normalized based on the % mass of PCL segments in the PCL-PDMS-PCL macromers. $\Delta H_m{}^0$ is 139.5 J/g for 100% crystalline PCL.[26]

^{1}H-NMR spectra of the copolymers were obtained on a Bruker 500 M spectrometer at 200 MHz. The spectrum was taken in deuterated chloroform at 20°C. The composition of copolymers was calculated from the ratios of absorbance at 0.07 and 4.05 ppm. Average molecular weight (Mn) was calculated according to the following equation:

$$M_n = M_{PCL} \times 40 + M_{PDMS} \times \left(\frac{40}{3}\right)\left(\frac{M}{N}\right) + M_{PCL} \times 40$$

In this equation, it was assumed that the synthesized copolymers had a constant number of PCL repeating units, $n = 40$ or 20, and the integration for methylene group in the ^{1}H-NMR spectrum from PCL repeating units is M and for methyl group in PDMS repeating units is N.

Fabrication of PCL-PDMS-PCL copolymer based microspheres

PCL-PDMS-PCL microspheres were fabricated using a reverse-phase precipitation method.[27] Briefly, after the copolymer synthesis reaction, the solution in 1,2-dichloromethane was slowly poured into a 1000 mL big beaker containing 500 mL methanol. Microspheres were formed and precipitated at the bottom of beaker when stirring the solution at 100 rpm for 2 h. Then the precipitate was filtrated to remove the mixture of 1,2-dichloromethane and methanol. To remove the remaining oligomers and tin (II) 2-ethylhexanoate, the filtrate was washed thrice with methanol. The final products were dried under vacuum for more than 24 h before characterizations or the use in cell culture.

Scanning electron microscopy

The morphology of microparticle samples was examined using field emission scanning electron microscope (SEM) (JEOL 7401F). Samples were sputter-coated with a thin layer of gold before observation. The SEM images were analyzed using ImageJ software to obtain the size distribution of microspheres.

Undifferentiated ESC cultures

Murine ES-D3 line (American Type Culture Collection, Manassas, VA) was maintained on six-well culture plates coated with 0.1% gelatin (Millipore, Temecula, CA) in a standard 5% CO_2 incubator.[28–31] The culture medium was composed of Dulbecco's modified Eagle's medium (DMEM; Invitrogen, Carlsbad, CA) supplemented with 10% ESC-screened fetal bovine serum (FBS; Hyclone, Logan, UT), 1 mM sodium pyruvate, 0.1 mM β-mercaptoethanol, penicillin (100 U/mL), streptomycin (100 μg/mL) (all from Invitrogen), and 1000 U/mL leukemia inhibitory factor (Millipore). The cells were seeded at $2–4 \times 10^4$ cells/cm^2 and subcultured every 2–3 days with 0.05% trypsin.

Cell seeding with microspheres and the induction for cardiovascular differentiation

For cell culture, PCL-PDMS-PCL microspheres were sterilized with 70% ethanol and then washed thrice with phosphate-buffered saline (PBS). Different types of microspheres (0.2 mg/mL) were mixed with the cells and seeded in low attachment 24-well plates at 2×10^5 cells in 1 mL of medium. The differentiation medium was composed of DMEM, 10% FBS, 1 mM β-mercaptoethanol, penicillin (100 U/mL), and streptomycin (100 μg/mL) (DMEM-FBS). The medium was supplemented with 10 ng/mL bone morphogenetic protein (BMP)-4 (R&D Systems) for the first 4 days. At day 4, the formed EBs with microspheres were replated into 24-well plates coated with 0.1% gelatin. The cells were fed with differentiation medium without growth factors. At day 2, 5, 11, and 14 after replating, the cells were characterized for cardiovascular markers. For culture medium experiments, the replated cells were maintained in either DMEM-FBS or RPMI-B27 (RPMI + 2% B27) serum-free medium (Invitrogen).

To illustrate the influence of elastic modulus only, the PCL-PDMS-PCL copolymers (9.3 kPa, 58 MPa, and 103 MPa) were processed into 2D disks (diameter: 10 mm, thickness: 1 mm). The day 4 EBs without particles were replated onto different 2D disks coated with 0.1% gelatin. The cells were grown for 11 days and characterized for cell proliferation and cardiovascular marker expression.

Biochemical assays

LIVE/DEAD® Staining Kit (Molecular Probes) was used to assess viability of the cells in EBs with microspheres.[32] After a 5-day culture, the samples were incubated in DMEM containing 1 μM calcein AM (green) and 2 μM ethidium homodimer I (red) for 30 min and imaged under a fluorescent microscope (Olympus IX70, Melville, NY). Cell numbers of microsphere cultures at day 1, 3, and 5 were determined using a hemocytometer after trypsinization. The cell aggregates with microspheres were also incubated with 5 mg/mL 3-(4,5-dimethylthiazol-2-yl)-2,5-diphenyltetrazolium bromide (MTT; Sigma) solution at day 1, 3, and 5 to evaluate metabolic activity. The absorbance of the samples was measured at 500 nm using a microplate reader (Bio-Rad, Richmond, CA).

Reverse transcription polymerase chain reaction

Total RNA was isolated from ESC samples using the RNeasy Mini Kit (QIAGEN, Valencia, CA) according to the manufacturer's protocol followed by the treatment of DNA-Free RNA Kit (Zymo, Irvine, CA).[33] Reverse transcription was carried out using 2 μg of total RNA, anchored oligo-dT primers (Operon, Huntsville, AL), and SuperScript III (Invitrogen, Carlsbad, CA) (according to the protocol of the manufacturer). Primers specific for target genes (Table 1) were designed using the software Oligo Explorer 1.2 (GeneLink, Hawthorne, NY, Table 1). The gene *β-actin* was used as an endogenous control for normalization of expression levels. Real-time reverse transcription polymerase chain reactions (RT-PCRs) were performed on an ABI7500 instrument (Applied Biosystems, Foster City, CA), using SYBR1 Green PCR Master Mix (Applied Biosystems). The amplification reactions were performed as follows: 2 min at

Table 1. Primer Sequence for Target Genes

Gene	*Forward primer 5′–3′*	*Reverse primer 5′–3′*
Oct-4	CAGCAGATCAGCCACATCGCC	TGAGAAAGGAGACCCAGCAGCC
Nanog	CCTGTGATTTGTGGGCCTG	GACAGTCTCCGTGTGAGGCAT
β-actin	GTACTCCGTGTGGATCGGCG	AAGCATTTGCGGTGGACGATGG

50°C, 10 min at 95°C, and 40 cycles of 95°C for 15 s and 55°C for 30 s, and 68°C for 30 s. Fold variation in gene expression was quantified by means of the comparative Ct method: $2^{-(C_{t\ treatment} - C_{t\ control})}$, which is based on the comparison of expression of the target gene (normalized to the endogenous control beta-actin) between day 4 EB samples and the day 0 undifferentiated cells.

Immunocytochemistry

Briefly, the cells were fixed with 4% paraformaldehyde (PFA) and permeabilized with 0.2–0.5% Triton X-100 (for intracellular markers only). The samples were then blocked and incubated with mouse or goat primary antibody against: KDR (Millipore), CD31 (PECAM-1) (Santa Cruz Biotechnology, Inc., Dallas, TX), VE-cadherin (Santa Cruz Biotechnology, Inc.), and α-actinin (Sigma). After washing, the cells were incubated with the corresponding secondary antibody (Molecular Probes): Alexa Fluor® 594 donkey anti-goat IgG (for CD31 and VE-cadherin) or Alexa Fluor® 488 goat anti-mouse IgG1 (for KDR and α-actinin). For F-actin staining, the cells were incubated with Alexa Fluor 594 Phalloidin (Molecular Probes). For Yes-associated protein (YAP) staining, the cells were incubated with rabbit primary antibody (Santa Cruz Biotechnology, Inc.), followed by Alexa Fluor 594 goat anti-rabbit IgG. The samples were stained with Hoechst 33342 (to reveal cell nuclei) and visualized under a fluorescent microscope.

Flow cytometry

To quantify cardiovascular marker expression, the cells were harvested by trypsinization and analyzed by flow cytometry.[34] Briefly, 1×10^6 cells per sample were fixed with 4% PFA and washed with staining buffer (2% FBS in PBS). The cells were permeabilized with 100% cold methanol (for intracellular markers only), blocked, and then incubated with primary antibodies against KDR, CD31 (PECAM-1), VE-cadherin, Nkx2.5 (Santa Cruz Biotechnology, Inc.), and α-actinin followed by the corresponding secondary antibody: Alexa Fluor 594 donkey anti-goat IgG (for CD31 and VE-cadherin), Alexa Fluor 594 goat anti-rabbit IgG (for Nkx2.5), or Alexa Fluor 488 goat anti-mouse IgG1 (for KDR and α-actinin). The cells were acquired with BD FACSCanto™ II flow cytometer (Becton Dickinson) and analyzed against isotype controls using FlowJo software.

Vascular structure assay

Briefly, 24-well plates were coated with 200 μL/well 1:1 diluted Geltrex (B&D Biosciences) at room temperature for more than 30 min. The cells were plated at 5×10^5 cells on Geltrex-coated plates in 500 μL EGM-2 medium (Lonza, for endothelial cells) and incubated at 37°C in 5% CO_2 for 7 days. Cell morphology was photographed by a phase-contrast microscope. The cells were then fixed and assessed for marker expression of CD31, VE-cadherin, and F-actin.

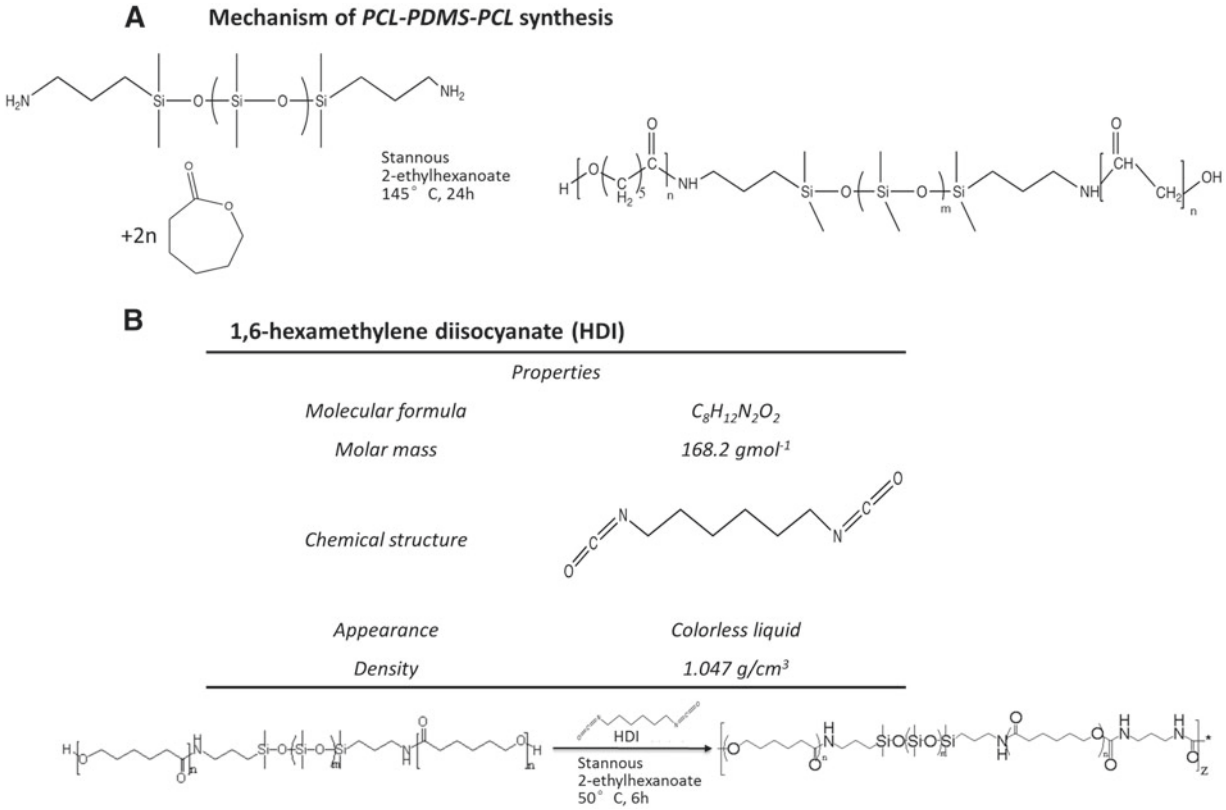

FIG. 1. Mechanism of PCL-PDMS-PCL copolymer synthesis. **(A)** Structure of PCL-PDMS-PCL macromers. Macromers of PCL_n-block-$PDMS_m$-block-PCL_n were synthesized by ring-opening polymerization of ε-caprolactone in the presence of $NH_2-PDMS_m-NH_2$ and tin-catalyst. **(B)** Structure of coupling agent HDI and the reaction in the presence of HDI. HDI, hexamethylene diisocyanate; PCL, poly-ε-caprolactone; PDMS, polydimethylsiloxane.

Table 2. Composition, Molecular Weight, and Thermal Properties of Different PCL-PDMS-PCL Copolymers

Copolymers	*Polymer 1*	*Polymer 2*	*Polymer 3*	*Polymer 4*
PCL (n)	40	40	40	20
PDMS (m)	28	34	58	58
Molecular weight (g/mol)	11,588	12,100	13,586	9100
Feed ratio	80/28	80/34	80/58	40/58
^{1}H-NMR ratio	80/31	80/37	80/57	40/50
Tm/°C ($n=3$)	57.8 ± 0.6	46.0 ± 0.7	56.9 ± 0.4	53.3 ± 0.6
Cryst. (%) ($n=3$)	41.9 ± 1.6	40.1 ± 1.5	35.2 ± 4.0[a]	25.8 ± 4.0[abc]

[a]p-Value <0.05 in comparison with polymer 1.
[b]p-Value <0.05 in comparison with polymer 2.
[c]p-Value <0.05 in comparison with polymer 3.

Statistical analysis

Each experiment was carried out at least thrice. The representative experiments were presented, and the results are expressed as mean ± standard deviation. To assess the statistical significance, one-way ANOVA followed by Fisher's LSD *post hoc* tests was performed. A p-value <0.05 was considered statistically significant.

Results

Fabrication and characterization of PCL-PDMS-PCL copolymers

Macromers of PCL_n-block-$PDMS_m$-block-PCL_n ($n=20$, 40, and 50, $m=10$, 34, 58, and 296) were synthesized by ring-opening polymerization of ε-caprolactone in the presence of $NH_2-PDMS_m-NH_2$ and tin-catalyst as shown in Figure 1.

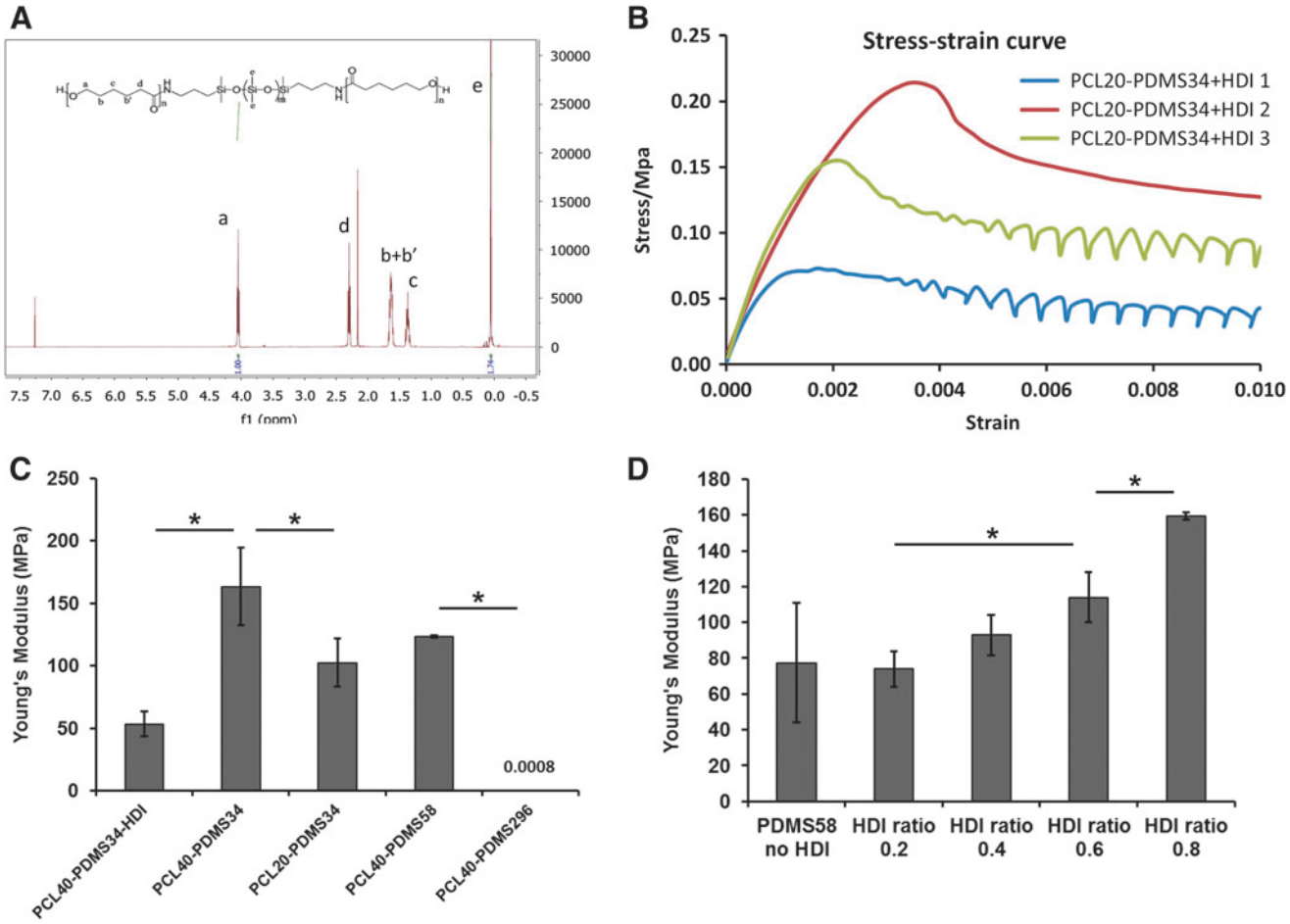

FIG. 2. Characterization of PCL-PDMS-PCL copolymers for chemical and mechanical properties. **(A)** Representative ^{1}H-NMR analysis of copolymer. **(B)** Representative stress–strain curve of copolymer. **(C)** The Young's modulus of PCL-PDMS-PCL copolymers with different PCL and PDMS lengths. **(D)** The Young's modulus of PCL-PDMS-PCL copolymers with different HDI ratio. *$p<0.05$. Color images available online at www.liebertpub.com/tec

Composition, molecular weight, and thermal properties of different PCL-PDMS-PCL copolymers were characterized (Table 2). ^{1}H-NMR analysis confirmed the feed ratio of the two polymers (Fig. 2A and Table 2). T_m of PCL-PDMS-PCL copolymer (46–57°C) was lower than the PCL (60°C). Decreasing the length of PCL segments showed the decrease in % of crystallinity (Table 2). Young's modulus of copolymers was measured by DMA, and the representative stress–strain curve was shown in Figure 2B. By varying the segments of PCL and PDMS, the copolymers displayed different elastic modulus (0.8 kPa–160 MPa) (Fig. 2C). HDI is used as a coupling agent to increase the chain length of copolymer. Higher modulus was observed when the ratio of HDI was increased (from 80 to 160 MPa for HDI ratio from 0 to 1) (Fig. 2D). These results confirm the properties of PCL-PDMS-PCL copolymers and demonstrate that elastic modulus of the copolymers can be tailored by varying hard segment (PCL) and soft segment (PDMS).

Effect of elastic modulus of PCL-PDMS-PCL copolymers

Before the evaluation of the copolymers, the differentiation media for cardiovascular differentiation of ESCs was compared. The differentiation was initiated with BMP-4 induction to obtain KDR^{+} progenitors which can further differentiate into cardiac cells and vascular cells (Fig. 3A). The day 4 EBs were replated onto the gelatin-coated surface in DMEM-FBS or RPMI-B27 medium. At day 3 after replating, KDR was expressed at a higher level for cells grown in DMEM-FBS compared

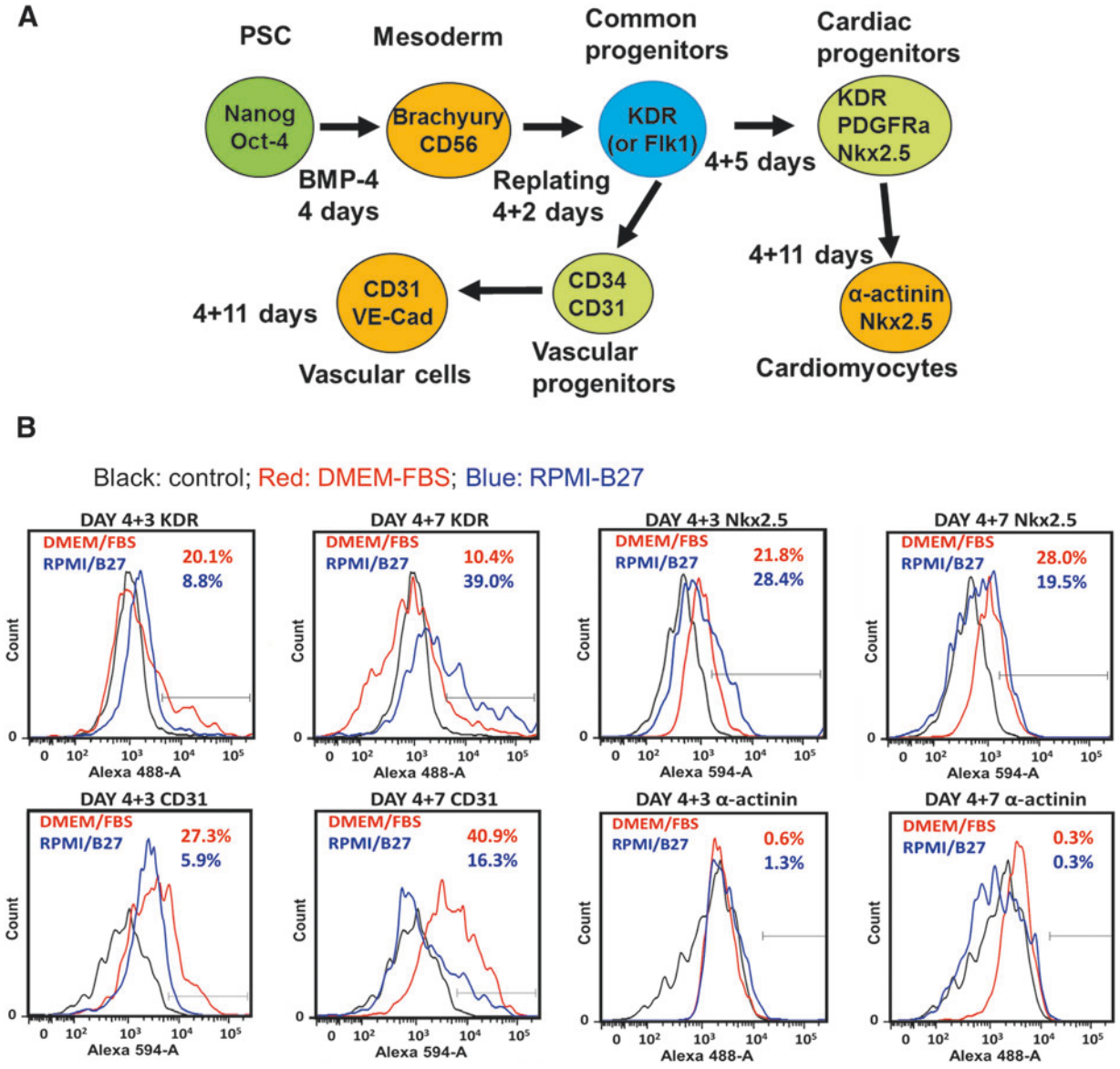

FIG. 3. Cardiovascular differentiation from ESCs. **(A)** Schematic illustration of cardiac and vascular differentiation from ESCs. **(B)** Representative flow cytometry histograms of cardiovascular marker expression in different media: DMEM plus 10% FBS (DMEM-FBS, shown in *red*) and RPMI plus 2% B27 serum replacement (RPMI-B27, shown in *blue*). The *black line* is negative control. DMEM, Dulbecco's modified Eagle's medium; ESCs, embryonic stem cells; FBS, fetal bovine serum. Color images available online at www.liebertpub.com/tec

to RPMI-B27 media (20.1% vs. 8.8% for DMEM-FBS or RPMI-B27, respectively), but decreased quickly at day 7 (10.4% vs. 39.0% for DMEM-FBS or RPMI-B27, respectively) (Fig. 3B). Compared to RPMI-B27 culture, CD31 expression was higher at both day 3 (27.3% vs. 5.9% for DMEM-FBS or RPMI-B27, respectively) and day 7 (40.9% vs. 16.3% for DMEM-FBS or RPMI-B27, respectively) for DMEM-FBS culture. For cardiac markers, Nkx2.5 level was higher for RPMI-B27 condition (28.4% vs. 21.8% for RPMI-B27 or DMEM-FBS, respectively) at day 3 after replating, but became lower (19.5% vs. 28.0% for RPMI-B27 or DMEM-FBS, respectively) than DMEM-FBS culture at day 7 after replating. Both cultures had comparable levels of α-actinin (0.3–1.3%). The temporal expression of KDR and Nkx2.5 (the progenitor markers) suggested that RPMI-B27 may need longer differentiation time than DMEM-FBS. Based on these results, DMEM-FBS medium was used in further study.

2D disks of three types of copolymer (PCL20-PDMS58-PCL20: 9.3 kPa, PCL40-PDMS28-PCL40: 58 MPa, and PCL20-PDMS34-PCL20+HDI: 103 MPa) were evaluated for cardiovascular differentiation (Fig. 4). The highest expression of vascular markers CD31 (63.5%) and VE-cadherin (56.5%) was observed for the 9.3 kPa condition (Fig. 4A). For 58 and 103 MPa conditions, the CD31 expression was 14.3% and 36.4%, respectively, and the VE-cadherin expression was 21.1% and 52.0%, respectively. The lower CD31 and VE-cadherin expression for 58 MPa condition than 103 MPa condition may be due to differentiation variations since vascular differentiation was shown to be promoted at the lower elastic modulus.[21,35,36] These data indicate that the modulus range of 58–103 MPa resulted in 14–36% CD31 and 21–52% VE-cadherin for EBs replated on the 2D disks. The expression level of α-actinin was similar (1.6–4.9%) for all three conditions. The fold increase in cell number was the lowest for the 9.3 kPa condition, but was similar for the modulus of 58 and

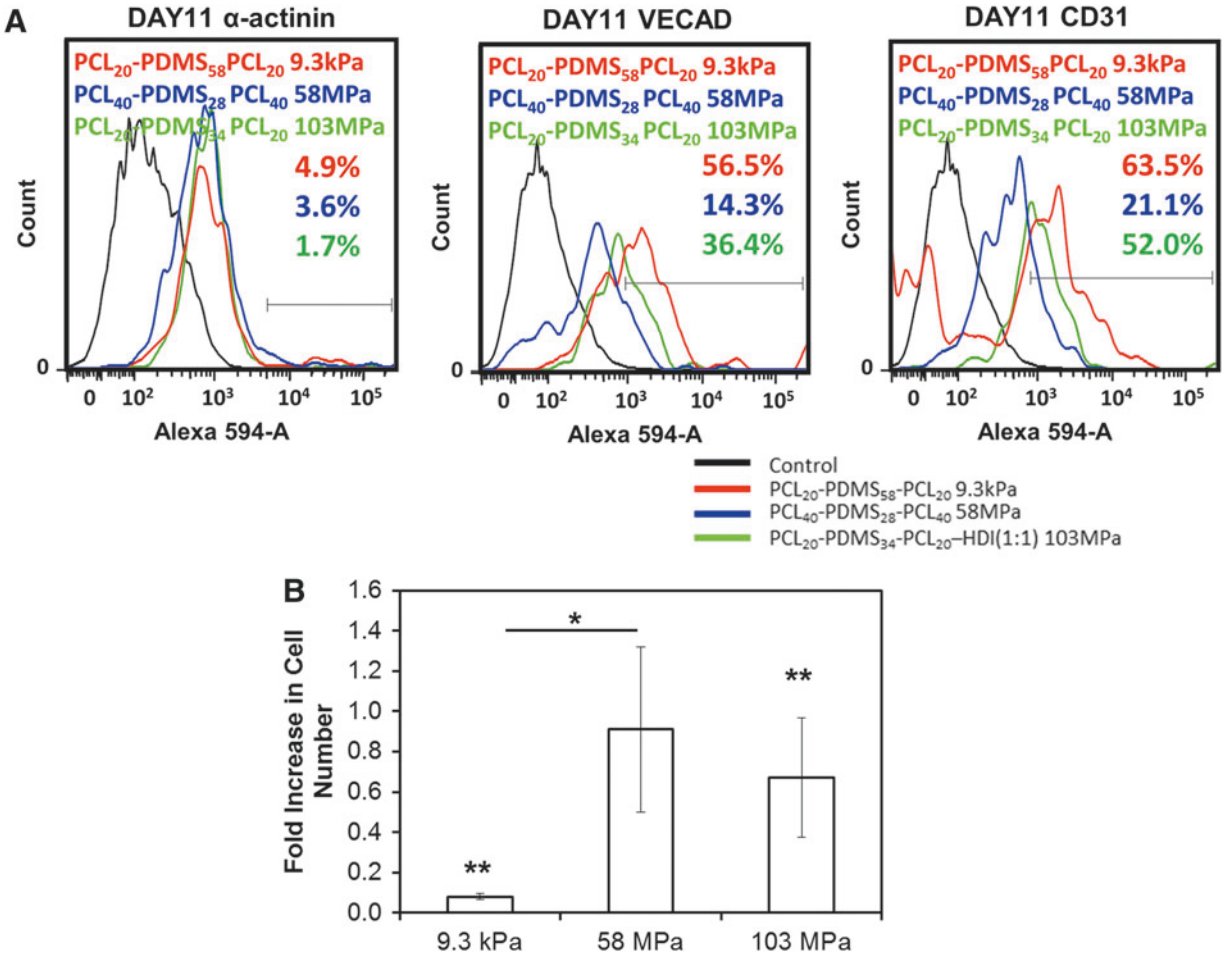

FIG. 4. Effect of elastic modulus of PCL-PDMS-PCL copolymer 2D disks on cell proliferation and cardiovascular differentiation. **(A)** Representative flow cytometry histograms of cardiovascular marker expression for PCL-PDMS-PCL copolymers with different elastic modulus. *Red*: PCL_{20}-$PDMS_{58}$-PCL_{20}-9.3 kPa; *blue*: PCL_{40}-$PDMS_{28}$-PCL_{40}-58 MPa; *green*: PCL_{20}-$PDMS_{34}$-PCL_{20}–HDI (1:1)-103 MPa; *black*: negative control. **(B)** Fold increase in cell number for cells grown on PCL-PDMS-PCL copolymers with different elastic modulus. $*p < 0.05$. $**p < 0.05$ between 9.3 kPa and 103 MPa conditions. Color images available online at www.liebertpub.com/tec

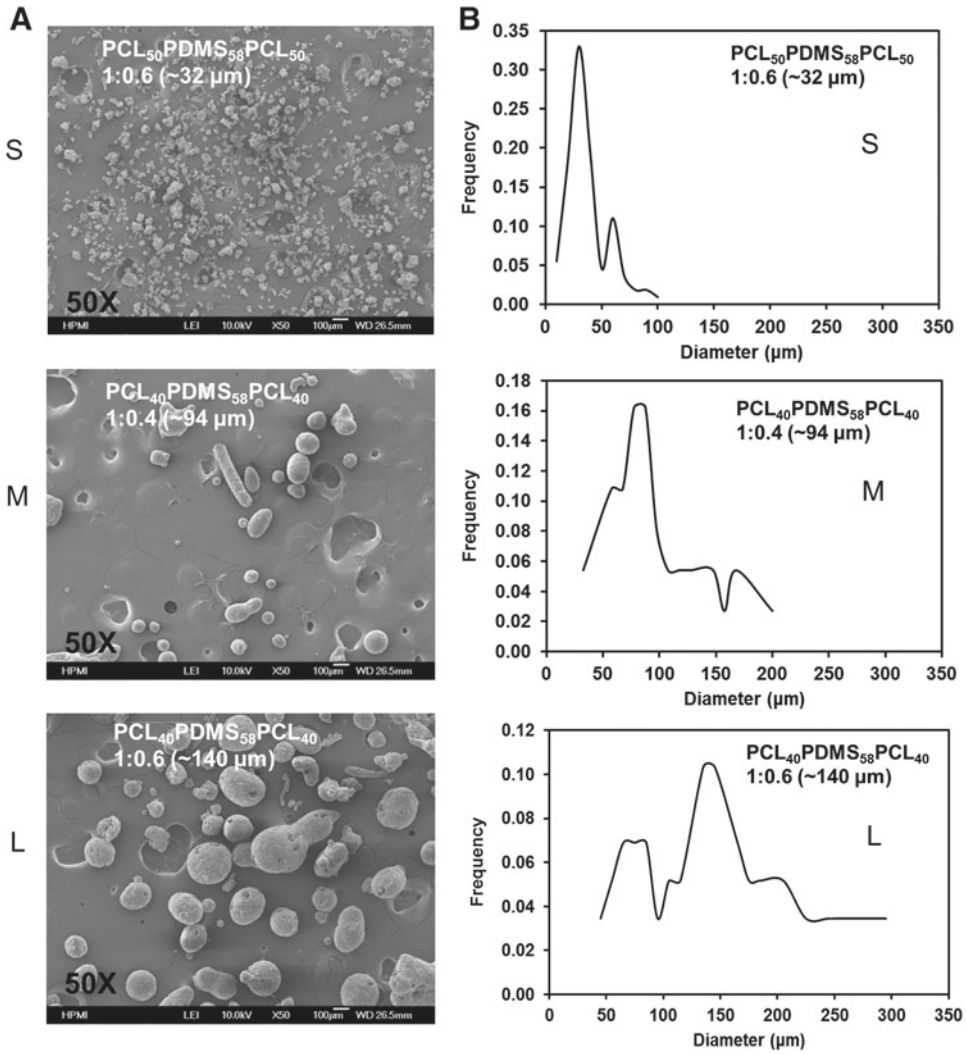

FIG. 5. Characterization of PCL-PDMS-PCL copolymer based microspheres. **(A)** Scanning electron microscopy images of PCL-PDMS-PCL microspheres. **(B)** Size distribution of the three types of PCL-PDMS-PCL microspheres. Based on the size distribution, the microspheres are named as S (small) ($n=94$), M (medium) ($n=37$), and L (large) ($n=58$).

103 MPa (Fig. 4B), indicating that the substrate with high modulus promotes cell proliferation.

Biocompatibility of PCL-PDMS-PCL microspheres

PCL-PDMS-PCL (with modulus range of 90–110 MPa) microspheres with three different sizes were then fabricated (Fig. 5). It was noticed that the soft 9.3 kPa copolymer was difficult for microsphere fabrication and the maintenance of sphere size. The morphology of the microspheres was shown in the SEM images, and the size distribution of microspheres was characterized. The average diameter of the three types of microspheres was 32 ± 11 μm (S), 94 ± 39 μm (M), and 140 ± 65 μm (L). After the microspheres (0.2 mg/mL) were mixed with ESCs for EB formation, the microspheres were incorporated into the EBs as shown in the phase contrast images (Fig. 6Ai). The percentages of EBs that incorporated with microspheres (showing as dark particles in the EBs) were assessed based on image analysis. About all the EBs contained the S-spheres, about 40% of EBs contained M-spheres, and about 25% of EBs contained L-spheres. The EBs incorporating the microspheres were viable as shown in the images of LIVE/DEAD assay (Fig. 6Aii). The dead cells were only observed for the single cells that were not able to form the EBs. MTT activity showed the increase with culture time for all three conditions, further confirming the viability of the cells in the EBs (Fig. 6B). M-sphere condition showed the highest level of MTT activity compared to S-sphere and L-sphere conditions. About fourfold increase in cell number was observed over 5-day culture for all the three groups (Fig. 6C). The BrdU expression of the replated cells was also evaluated (Supplementary Fig. S1; Supplementary Data are available online at www.liebertpub.com/tec). About 42% $BrdU^+$ cells for S-sphere, 31% for M-sphere, and 35% for L-sphere condition were observed. All these data demonstrate the biocompatibility of PCL-PDMS-PCL microspheres when incorporating with the EBs.

Cardiovascular differentiation of ESCs grown with microspheres

The EBs incorporating the microspheres were evaluated for the gene expression of *Oct-4* and *Nanog* (Table 3). The decrease of *Oct-4* and *Nanog* indicated the loss of pluripotency for the differentiated cells. The cells were further

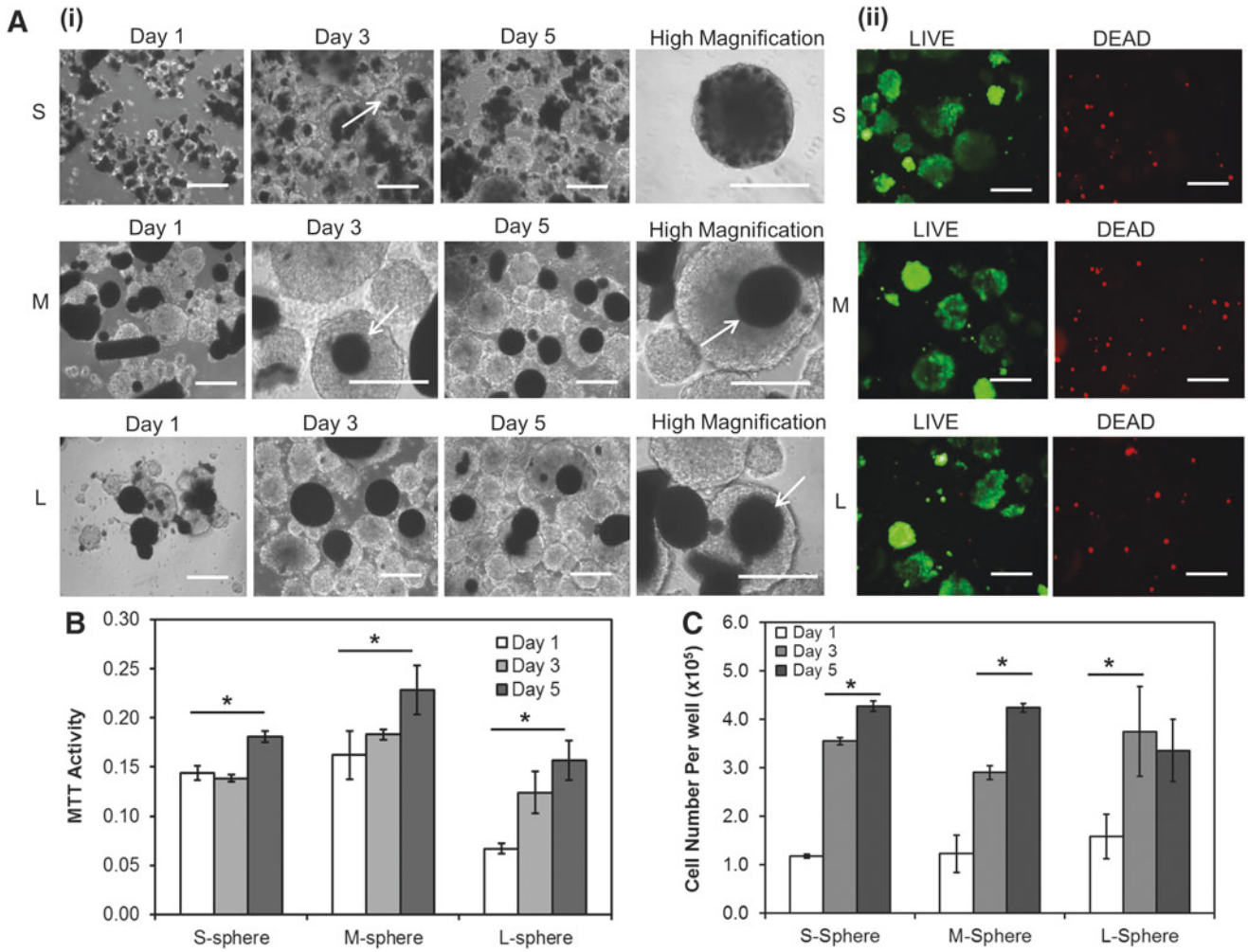

FIG. 6. Incorporation of PCL-PDMS-PCL microspheres with EBs. **(A) (i)** Phase contrast images of EBs with microspheres at different days; **(ii)** cell viability determined by LIVE/DEAD assay; scale bar: 200 μm. The *white arrows* indicate the black microspheres inside the EBs. **(B)** MTT activity; **(C)** cell number kinetics. $*p < 0.05$. EBs, embryoid bodies. Color images available online at www.liebertpub.com/tec

replated and grown for 11–15 days toward cardiovascular differentiation. At the end of differentiation, the cells expressed CD31 and VE-cadherin but less α-actinin (Fig. 7A). The quantification of progenitor marker showed the high expression of KDR (69.1% ± 3.0% vs. 25.0% ± 9.1% or 26.8% ± 21.3%) at day 3 for S-sphere condition compared to M- and L-sphere conditions. However, the M-sphere condition showed the highest expression of CD31 (67.0% ± 6.0% vs. 29.3% ± 9.3% for S group or 29.9% ± 18.1% for L group) and VE-cadherin (65.5% ± 13.6% vs. 32.8% ± 6.1% for S group or 19.1% ± 9.0% for L group) at day 11 after replating (Fig. 7B, C). For the differentiation in the absence of microspheres, the cells had 53.7% ± 16.1% $CD31^+$ and 17.1% ± 6.6% VE-$cadherin^+$ populations, which were comparable to S and M groups (Supplementary Fig. S2). Since cardiac marker α-actinin expression was low again (3.69% ± 0.04% for EBs without microspheres in Supplementary Fig. S2 and 1.7–4.5% for EBs containing microspheres in Supplementary Fig. S3), the differentiation protocol was more prone to vascular differentiation. The expression of F-actin and YAP was examined for the replated cells of the three groups (Supplementary Fig. S4). The cells expressed the actin stress fibers and nuclear pattern of YAP for all three groups, but no significant difference in expression pattern among different groups was observed.

TABLE 3. THE EXPRESSION OF OCT-4 AND NANOG IN DAY 4 EMBRYOID BODIES INCORPORATING MICROSPHERES

Culture conditions	*Oct-4*	*Nanog*
S-sphere	0.66 ± 0.04	0.95 ± 0.05
M-sphere	0.60 ± 0.07	0.17 ± 0.17[a]
L-sphere	0.75 ± 0.06	0.37 ± 0.15[a]

[a]*p*-Value <0.05 in comparison with S-sphere.

The differentiated cells were also harvested and replated onto Geltrex-coated surface in endothelial cell growth medium and growth factors. Under endothelial cell growth condition, CD31 and VE-cadherin positive populations were enriched (Fig. 8). Elongated endothelial cell-like morphology was observed and the M-sphere condition showed more branching points.

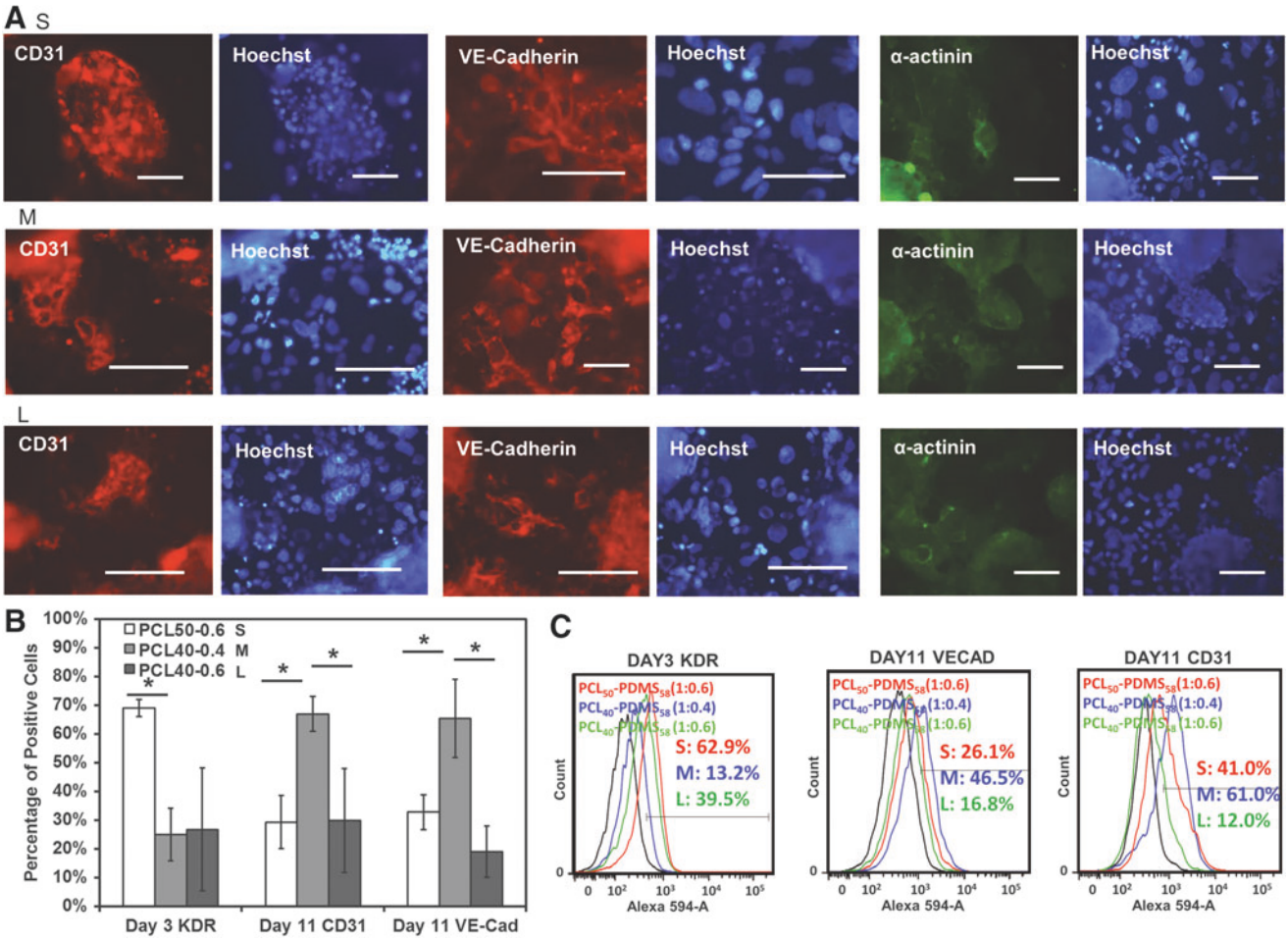

FIG. 7. Cardiovascular differentiation from EBs containing PCL-PDMS-PCL microspheres. **(A)** Immunocytochemistry analysis of cardiovascular markers CD31, VE-cadherin, and α-actinin expression in the cells differentiated from EBs incorporated with microspheres; scale bar: 100 μm. **(B)** Flow cytometry analysis of KDR, CD31, and VE-cadherin expression of cells differentiated from EBs incorporated with microspheres ($n=3$). $*p<0.05$. **(C)** Representative flow cytometry histograms of cardiovascular marker expression for conditions of different microspheres. *Red*: S-sphere, PCL_{50}-$PDMS_{58}$-PCL_{50} (1:0.6); *blue*: M-sphere, PCL_{40}-$PDMS_{58}$-PCL_{40} (1:0.4); *green*: L-sphere, PCL_{40}-$PDMS_{58}$-PCL_{40} (1:0.6); *black*: negative control. Color images available online at www.liebertpub.com/tec

Discussion

Complex and interactive niche signals, including the mechanical and topographical cues, play a critical role in stem cell lineage commitment.[37] The microstructures and elastic properties of microscale spheres, particles, ribbons, or scaffolds have shown the influence on stem cell fate decisions and drawn attentions in biomaterial design and characterizations.[16,38] In this study, PCL-PDMS-PCL copolymers were synthesized, characterized, and used for regulating cardiovascular differentiation from ESCs. In particular, biophysical properties, including microsphere size and elastic modulus of PCL-PDMS-PCL copolymers, were studied.

PCL-PDMS-PCL copolymers are suitable for fabricating thermoresponsive shape memory substrates/scaffolds for various biomedical applications.[39] The use of PCL and PDMS also enables the tuning of elastic properties of the materials by varying the ratio of PCL segments and PDMS segments. This study successfully synthesized PCL-PDMS-PCL copolymers with different PCL and PDMS segments, which were characterized by ^{1}H-NMR, DSC, and DMA. Increasing PDMS segment length decreased the elastic modulus, while increasing PCL segment length increased the elastic modulus. The elastic properties of PCL-PDMS-PCL copolymers can be further tuned using HDI coupling agent. Potentially, PCL-PDMS-PCL copolymers can be modified with other materials depending on the purpose of the study. For example, tri-block PCL-PDMS-PCL can be copolymerized with DL-lactic acid to control the degradation rate.[40]

The influence of PCL-PDMS-PCL copolymers on cardiovascular differentiation in 2D culture was evaluated using 2D disks with different elastic modulus. The effect was mainly observed for vascular differentiation rather than cardiac differentiation. Consistent with the reports from the literature that evaluated other materials,[21,36] soft PCL-PDMS-PCL copolymers (<10 kPa) promoted vascular differentiation compared to the hard copolymers (>50 MPa). These results demonstrate the feasibility of using PCL-PDMS-PCL copolymers in a biological system to regulate stem cell differentiation.

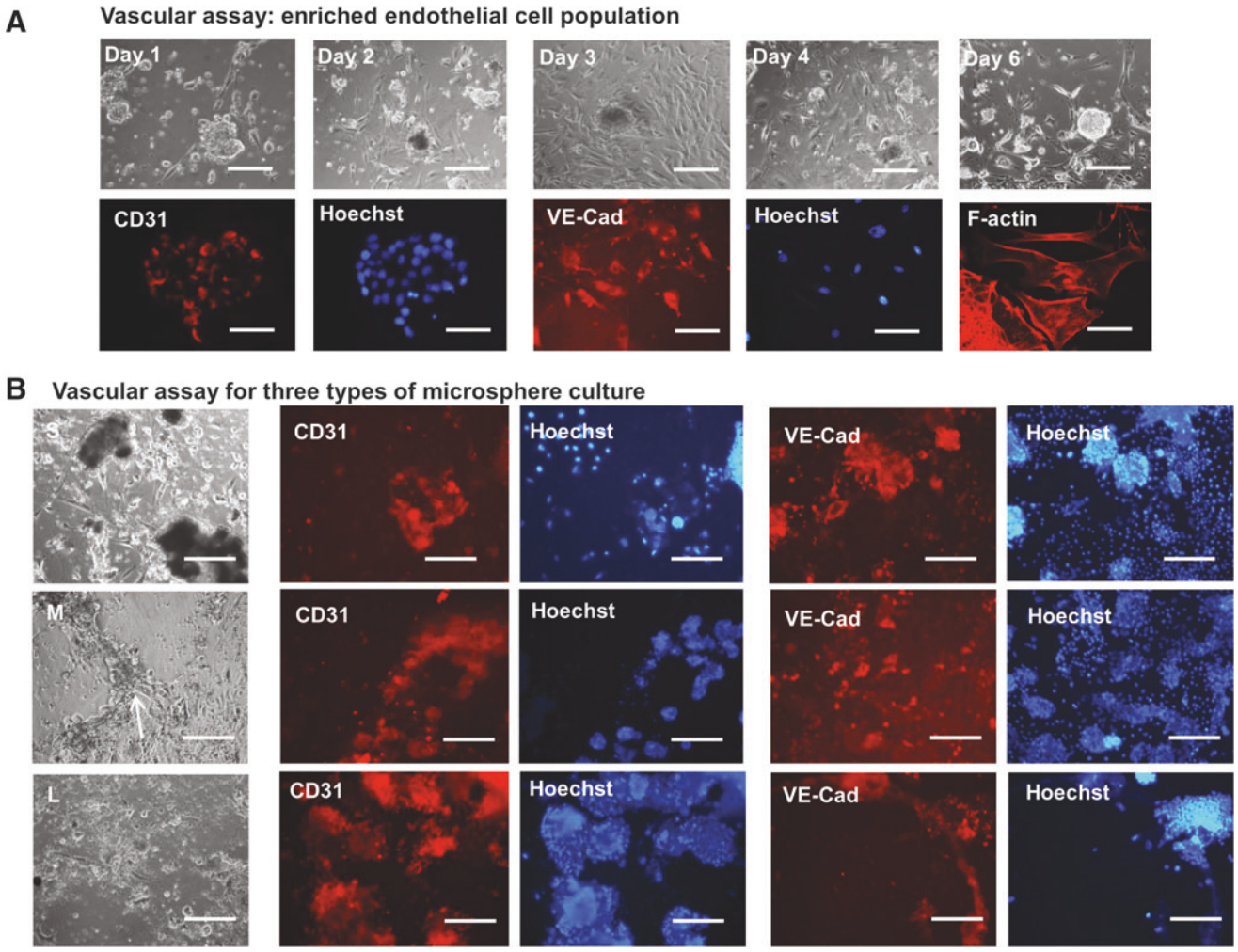

FIG. 8. Vascular network assay for the cells derived from EBs incorporating different PCL-PDMS-PCL microspheres. **(A)** Morphology of vascular cells derived from EBs grown in endothelial cell medium and the enrichment of vascular marker expression; fluorescent images were taken for day 7 culture. Phase contrast images, scale bar: 100 μm; fluorescent images, scale bar: 50 μm. **(B)** Vascular cells grown in the endothelial cell medium for the cells from EBs incorporated with different microspheres. Scale bar: 100 μm. The *white arrow* indicates vascular branch. Color images available online at www.liebertpub.com/tec

The influence of PCL-PDMS-PCL copolymers on cardiovascular differentiation in 3D culture was evaluated using microspheres with different sizes. While PCL-PDMS-PCL copolymers with tunable physical and thermal properties have been recently studied,[20,25] the use of such copolymers in stem cell culture has not been well reported. The PCL-PDMS-PCL microspheres were readily incorporated with the EBs and showed the biocompatibility during cardiovascular differentiation of ESCs. The EBs incorporating PCL-PDMS-PCL microspheres displayed high viability, normal MTT activity, and the proliferation activities.

In this study, differential expression of vascular markers was observed for the EBs incorporating the PCL-PDMS-PCL microspheres with different sizes. Higher KDR expression was found for the S-sphere group, but higher CD31 and VE-cadherin were observed for the M-sphere group. It is thought that stiffening EBs with microspheres contribute to the differential expression of vascular markers. Incorporation of gelatin microparticles with stem cell aggregates has shown to increase the stiffness of the aggregates by three to fourfold than those without microparticles.[41] Stiff substrates or scaffolds were reported to favor the early-stage mesoderm commitment from PSCs. For example, elastic modulus of the scaffolds differentially enhanced mesoderm (6 MPa), endoderm (1 MPa), or ectoderm (0.1 MPa) differentiation from human ESCs.[42] Similarly, when increasing the stiffness from 78 kPa to 1.2 MPa, mesoderm differentiation of human ESCs was promoted compared to endoderm differentiation.[43] In this study, the EBs with S-spheres had the highest frequency of microsphere incorporation and almost all the aggregates were stiffened with the microspheres, which may promote mesoderm commitment. M-sphere condition had less frequency of microsphere incorporation followed by the L-sphere condition. The higher CD31 and VE-cadherin expression for M-sphere condition may suggest the balanced mesoderm commitment and further differentiation into vascular lineage.

The effect of microsphere/microparticle size has been observed in the range of 0.24–25 μm for PLGA. The particle

size less than 1 μm (e.g., 0.24 μm) was found to be easily taken up by the cells through endocytosis, while microparticles with the size of 6 μm were more universally dispersed in the EBs compared to 25 μm microparticles.[11] The comparison of different particle sizes (1–11 μm) also showed complete cystic EBs when delivering RA using smaller size particle (1 μm).[14] This study revealed the influence of PCL-PDMS-PCL microspheres in the size range of 30–140 μm during ESC mesodermal differentiation.

Both Rho GTPase signaling and Hippo/YAP signaling have been investigated as the mechanotransduction sensors for stem cells.[44–46] The soft matrix leads to the cytoplasmic expression of YAP and the increased ability of the cells to form branching endothelial morphology.[21] It was found that stress fibers reduced YAP phosphorylation and promoted nuclear YAP accumulation; thus, disruption of stress fibers using cytochalasin D reduced nuclear YAP.[47] However, in this study, the replated cells with different microspheres all had nuclear expression of YAP, which suggested that the difference in differentiation should result from the suspension stage (e.g., EB culture) of differentiation, where EBs were incorporated with microspheres with different frequencies.

The microspheres are usually used as the carriers (<50 μm) to deliver the drugs or growth factors or as scaffolds or microcarriers (100–200 μm) to influence stem cell differentiation.[15,48] Delivery of BMP-4 through gelatin microspheres/microparticles more efficiently increased gene expression of mesoderm and ectoderm lineages because the BMP-4 loaded microparticles were able to use 12-fold less growth factor compared to soluble BMP-4 delivery.[10] Heparin microparticles allowed the delivery of heparin-bounding growth factors BMP-2, vascular endothelial growth factor, and fibroblast growth factor-2,[49] which stimulated the alkaline phosphatase activity of skeletal myoblasts and increased the DNA content mediated by cell particle contact. Similarly, the PCL-PDMS-PCL copolymer-based microspheres can be used as drug carriers and tissue engineering scaffolds as shown for PCL-based microspheres.[17,50] Compared with PCL polymer, PCL-PDMS-PCL copolymers have shape memory property that requires further investigation to design smart materials for regulating stem cell fate decisions. As the initial step to apply highly functional materials in stem cell cultures, the present study highlights the importance of biophysical properties of the PCL-PDMS-PCL microspheres during stem cell lineage commitment.

Conclusions

This study synthesized and characterized the biodegradable copolymers that comprised PCL hard segments and PDMS soft segments of variable lengths. The PCL-PDMS-PCL copolymers were evaluated as the substrates and the microspheres that supported cardiovascular differentiation of ESCs. PCL-PDMS-PCL copolymers displayed biocompatibility in ESC differentiation. Small size of microspheres induced higher expression of mesoderm progenitor marker KDR, while medium size of microspheres resulted in higher expression of vascular markers CD31 and VE-cadherin. This study demonstrates the influence of biophysical properties of PCL-PDMS-PCL copolymers on stem cell lineage commitment at the interface of biomaterials and stem cells.

Acknowledgments

The authors thank Ms. Ruth Didier in FSU Department of Biomedical Sciences for her help in flow cytometry analysis and Dr. B.K. Washburn and K. Poduch in FSU Department of Biological Sciences for their help with RT-PCR analysis. This work is supported by FSU start up fund, FSU CRC planning grant, and partially National Science Foundation (grant No. 1652992 to Y.L.).

Disclosure Statement

No competing financial interests exist.

References

1. Go, A.S., Mozaffarian, D., Roger, V.L., Benjamin, E.J., Berry, J.D., Blaha, M.J., Dai, S., Ford, E.S., Fox, C.S., Franco, S., Fullerton, H.J., Gillespie, C., Hailpern, S.M., Heit, J.A., Howard, V.J., Huffman, M.D., Judd, S.E., Kissela, B.M., Kittner, S.J., Lackland, D.T., Lichtman, J.H., Lisabeth, L.D., Mackey, R.H., Magid, D.J., Marcus, G.M., Marelli, A., Matchar, D.B., McGuire, D.K., Mohler, E.R., 3rd, Moy, C.S., Mussolino, M.E., Neumar, R.W., Nichol, G., Pandey, D.K., Paynter, N.P., Reeves, M.J., Sorlie, P.D., Stein, J., Towfighi, A., Turan, T.N., Virani, S.S., Wong, N.D., Woo, D., and Turner, M.B. Executive summary: heart disease and stroke statistics—2014 update: a report from the American Heart Association. Circulation **129,** 399, 2014.
2. Sharma, A., Burridge, P.W., McKeithan, W.L., Serrano, R., Shukla, P., Sayed, N., Churko, J.M., Kitani, T., Wu, H., Holmstrom, A., Matsa, E., Zhang, Y., Kumar, A., Fan, A.C., Del Alamo, J.C., Wu, S.M., Moslehi, J.J., Mercola, M., and Wu, J.C. High-throughput screening of tyrosine kinase inhibitor cardiotoxicity with human induced pluripotent stem cells. Sci Transl Med **9,** (377), 2017.
3. Belair, D.G., Whisler, J.A., Valdez, J., Velazquez, J., Molenda, J.A., Vickerman, V., Lewis, R., Daigh, C., Hansen, T.D., Mann, D.A., Thomson, J.A., Griffith, L.G., Kamm, R.D., Schwartz, M.P., and Murphy, W.L. Human vascular tissue models formed from human induced pluripotent stem cell derived endothelial cells. Stem Cell Rev **11,** 511, 2015.
4. Yang, L., Soonpaa, M.H., Adler, E.D., Roepke, T.K., Kattman, S.J., Kennedy, M., Henckaerts, E., Bonham, K., Abbott, G.W., Linden, R.M., Field, L.J., and Keller, G.M. Human cardiovascular progenitor cells develop from a KDR+ embryonic-stem-cell-derived population. Nature **453,** 524, 2008.
5. Kusuma, S., Shen, Y.I., Hanjaya-Putra, D., Mali, P., Cheng, L., and Gerecht, S., Self-organized vascular networks from human pluripotent stem cells in a synthetic matrix. Proc Natl Acad Sci U S A **110,** 12601, 2013.
6. Kohler, E.E., Wary, K.K., Li, F., Chatterjee, I., Urao, N., Toth, PT., Ushio-Fukai, M., Rehman, J., Park, C., and Malik, A.B. Flk1+ and VE-cadherin+ endothelial cells derived from iPSCs recapitulates vascular development during differentiation and display similar angiogenic potential as ESC-derived cells. PLoS One **8,** e85549, 2013.
7. Xu, C., Police, S., Hassanipour, M., Li, Y., Chen, Y., Priest, C., O'Sullivan, C., Laflamme, M.A., Zhu, W.Z., Van Biber, B., Hegerova, L., Yang, J., Delavan-Boorsma, K., Davies, A., Lebkowski, J., and Gold, J.D. Efficient generation and cryopreservation of cardiomyocytes derived from human embryonic stem cells. Regen Med **6,** 53, 2011.

8. Birket, M.J., Ribeiro, M.C., Verkerk, A.O., Ward, D., Leitoguinho, A.R., den Hartogh, S.C., Orlova, V.V., Devalla, H.D., Schwach, V., Bellin, M., Passier, R., and Mummery, C.L. Expansion and patterning of cardiovascular progenitors derived from human pluripotent stem cells. Nat Biotechnol **33,** 970, 2015.
9. Jha, R., Wu, Q., Singh, M., Preininger, M.K., Han, P., Ding, G., Cho, H.C., Jo, H., Maher, K.O., Wagner, M.B., and Xu, C. Simulated microgravity and 3D culture enhance induction, viability, proliferation and differentiation of cardiac progenitors from human pluripotent stem cells. Sci Rep **6,** 30956, 2016.
10. Bratt-Leal, A.M., Nguyen, A.H., Hammersmith, K.A., Singh, A., and McDevitt, T.C. A microparticle approach to morphogen delivery within pluripotent stem cell aggregates. Biomaterials **34,** 7227, 2013.
11. Ferreira, L., Squier, T., Park, H., Choe, H., Kohane, D.S., and Langer, R. Human embryoid bodies contaning nano- and microparticulate delivery vehicles. Adv Mater **20,** 2285, 2008.
12. Chen, A., Ting, S., Seow, J., Reuveny, S., and Oh, S. Considerations in designing systems for large scale production of human cardiomyocytes from pluripotent stem cells. Stem Cell Res Ther **5,** 12, 2014.
13. Bratt-Leal, A.M., Carpenedo, R.L., Ungrin, M.D., Zandstra, P.W., and McDevitt, T.C. Incorporation of biomaterials in multicellular aggregates modulates pluripotent stem cell differentiation. Biomaterials **32,** 48, 2011.
14. Carpenedo, R.L., Seaman, S.A., and McDevitt, T.C. Microsphere size effects on embryoid body incorporation and embryonic stem cell differentiation. J Biomed Mater Res A **94,** 466, 2010.
15. Singh, M., Sandhu, B., Scurto, A., Berkland, C., and Detamore, M.S. Microsphere-based scaffolds for cartilage tissue engineering: using subcritical CO(2) as a sintering agent. Acta Biomater **6,** 137, 2017.
16. DeVolder, R.J., Kim, I.W., Kim, E.S., and Kong, H. Modulating the rigidity and mineralization of collagen gels using poly(lactic-co-glycolic acid) microparticles. Tissue Eng Part A **18,** 1642, 2012.
17. Sinha, V.R., Bansal, K., Kaushik, R., Kumria, R., and Trehan, A. Poly-epsilon-caprolactone microspheres and nanospheres: an overview. Int J Pharm **278,** 1, 2004.
18. Dash, T.K., and Konkimalla, V.B. Poly-small je, Ukrainian-caprolactone based formulations for drug delivery and tissue engineering: a review. J Control Release **158,** 15, 2012.
19. Niu, Y., Chen, K.C., He, T., Yu, W., Huang, S., and Xu, K. Scaffolds from block polyurethanes based on poly(varepsilon-caprolactone) (PCL) and poly(ethylene glycol) (PEG) for peripheral nerve regeneration. Biomaterials **35,** 4266, 2014.
20. Zhang, D., Petersen, K.M., and Grunlan, M.A. Inorganic-organic shape memory polymer (SMP) foams with highly tunable properties. ACS Appl Mater Interfaces **5,** 186, 2013.
21. Mosqueira, D., Pagliari, S., Uto, K., Ebara, M., Romanazzo, S., Escobedo-Lucea, C., Nakanishi, J., Taniguchi, A., Franzese, O., Di Nardo, P., Goumans, M.J., Traversa, E., Pinto-do, O.P., Aoyagi, T., and Forte, G. Hippo pathway effectors control cardiac progenitor cell fate by acting as dynamic sensors of substrate mechanics and nanostructure. ACS Nano **8,** 2033, 2014.
22. Serrano, M.C., and Ameer, G.A. Recent insights into the biomedical applications of shape-memory polymers. Macromol Biosci **12,** 1156, 2012.
23. Tseng, L.F., Mather, P.T., and Henderson, J.H. Shape-memory-actuated change in scaffold fiber alignment directs stem cell morphology. Acta Biomater **9,** 8790, 2013.
24. Bejoy, J., Song, L., Zhou, Y., and Li, Y. Wnt-YAP interactions during neural tissue patterning of human induced pluripotent stem cells. Tissue Eng Part A 2017 [Epub ahead of print]; DOI:10.1089/ten.TEA.2017.0153.
25. Zhang, D., Giese, M.L., Prukop, S.L., and Grunlan, M.A. PCL-based shape memory polymers with variable PDMS Soft segment lengths. J Polym Sci A Polym Chem **49,** 754, 2011.
26. Pitt, C.G., Gratzl, M.M., Kimmel, G.L., Surles, J., and Schindler, A. Aliphatic polyesters II. The degradation of poly (DL-lactide), poly (epsilon-caprolactone), and their copolymers in vivo. Biomaterials **2,** 215, 1981.
27. Cai, T., Li, M., Zhang, B., Neoh, K.-G., and Kang, E.-T. Hyperbranched polycaprolactone-click-poly(N-vinylcaprolactam) amphiphilic copolymers and their applications as temperature-responsive membranes. J Mater Chem B **2,** 814, 2014.
28. Sart, S., Liu, Y., Ma, T., and Li, Y. Microenvironment regulation of pluripotent stem cell-derived neural progenitor aggregates by human mesenchymal stem cell secretome. Tissue Eng Part A **20,** 2666, 2014.
29. Sart, S., Ma, T., and Li, Y. Extracellular matrices decellularized from embryonic stem cells maintained their structure and signaling specificity. Tissue Eng Part A **20,** 54, 2014.
30. Sart, S., Yan, Y., Li, Y., Lochner, E., Zeng, C., Ma, T., and Li, Y. Crosslinking of extracellular matrix scaffolds derived from pluripotent stem cell aggregates modulates neural differentiation. Acta Biomater **30,** 222, 2016.
31. Yan, Y., Li, Y., Song, L., Zeng, C., and Li, Y. Pluripotent stem cell expansion and neural differentiation in 3-D scaffolds of tunable Poisson's ratio. Acta Biomater **49,** 192, 2017.
32. Sart, S., Yan, Y., and Li, Y. The microenvironment of embryoid bodies modulated the commitment to neural lineage post-cryopreservation. Tissue Eng Part C Methods **21,** 356, 2015.
33. Song, L., Wang, K., Li, Y., and Yang, Y. Nanotopography promoted neuronal differentiation of human induced pluripotent stem cells. Colloids Surf B Biointerfaces **148,** 49, 2016.
34. Yan, Y., Martin, L., Bosco, D., Bundy, J., Nowakowski, R., Sang, Q.X., and Li, Y. Differential effects of acellular embryonic matrices on pluripotent stem cell expansion and neural differentiation. Biomaterials **73,** 231, 2015.
35. Hanjaya-Putra, D., Yee, J., Ceci, D., Truitt, R., Yee, D., and Gerecht, S. Vascular endothelial growth factor and substrate mechanics regulate in vitro tubulogenesis of endothelial progenitor cells. J Cell Mol Med **14,** 2436, 2010.
36. Shkumatov, A., Baek, K., and Kong, H. Matrix rigidity-modulated cardiovascular organoid formation from embryoid bodies. PLoS One **9,** e94764, 2014.
37. Li, Z., Gong, Y., Sun, S., Du, Y., Lu, D., Liu, X., and Long, M. Differential regulation of stiffness, topography, and dimension of substrates in rat mesenchymal stem cells. Biomaterials **34,** 7616, 2013.
38. Han, L.H., Tong, X., and Yang, F. Photo-crosslinkable PEG-based microribbons for forming 3D macroporous scaffolds with decoupled niche properties. Adv Mater **26,** 1757, 2014.
39. Friess, F., Nochel, U., Lendlein, A., and Wischke, C. Polymer micronetworks with shape-memory as future

platform to explore shape-dependent biological effects. Adv Healthc Mater **3,** 1986, 2014.
40. Kayaman-Apohana, N., Karal-Yılmaza, O., Baysalc, K., and Baysal, B.M. Poly(dl-lactic acid)/triblock PCL–PDMS–PCL copolymers: synthesis, characterization and demonstration of their cell growth effects in vitro. Polymer **42,** 4109, 2001.
41. Baraniak, P.R., Cooke, M.T., Saeed, R., Kinney, M.A., Fridley, K.M., and McDevitt, T.C. Stiffening of human mesenchymal stem cell spheroid microenvironments induced by incorporation of gelatin microparticles. J Mech Behav Biomed Mater **11,** 63, 2012.
42. Zoldan, J., Karagiannis, E.D., Lee, C.Y., Anderson, D.G., Langer, R., and Levenberg, S. The influence of scaffold elasticity on germ layer specification of human embryonic stem cells. Biomaterials **32,** 9612, 2011.
43. Eroshenko, N., Ramachandran, R., Yadavalli, V.K., and Rao, R.R. Effect of substrate stiffness on early human embryonic stem cell differentiation. J Biol Eng **7,** 7, 2013.
44. Dupont, S., Morsut, L., Aragona, M., Enzo, E., Giulitti, S., Cordenonsi, M., Zanconato, F., Le Digabel, J., Forcato, M., Bicciato, S., Elvassore, N., and Piccolo, S. Role of YAP/TAZ in mechanotransduction. Nature **474,** 179, 2011.
45. McBeath, R., Pirone, D.M., Nelson, C.M., Bhadriraju, K., and Chen, C.S. Cell shape, cytoskeletal tension, and RhoA regulate stem cell lineage commitment. Dev Cell **6,** 483, 2004.
46. Yang, C., Tibbitt, M.W., Basta, L., and Anseth, K.S. Mechanical memory and dosing influence stem cell fate. Nat Mater **13,** 645, 2014.
47. Wada, K., Itoga, K., Okano, T., Yonemura, S., and Sasaki, H. Hippo pathway regulation by cell morphology and stress fibers. Development **138,** 3907, 2011.
48. Nguyen, A.H., Wang, Y., White, D.E., Platt, M.O., and McDevitt, T.C. MMP-mediated mesenchymal morphogenesis of pluripotent stem cell aggregates stimulated by gelatin methacrylate microparticle incorporation. Biomaterials **76,** 66, 2015.
49. Hettiaratchi, M.H., Miller, T., Temenoff, J.S., Guldberg, R.E., and McDevitt, T.C. Heparin microparticle effects on presentation and bioactivity of bone morphogenetic protein-2. Biomaterials **35,** 7228, 2014.
50. Luciani, A., Coccoli, V., Orsi, S., Ambrosio, L., and Netti, P.A. PCL microspheres based functional scaffolds by bottom-up approach with predefined microstructural properties and release profiles. Biomaterials **29,** 4800, 2008.

Address correspondence to:
Yan Li, PhD
Department of Chemical and Biomedical Engineering
FAMU-FSU College of Engineering
Florida State University
2525 Pottsdamer Street, A131
Tallahassee, FL 32310

E-mail: yli@eng.fsu.edu

Received: June 26, 2017
Accepted: August 21, 2017
Online Publication Date: September 28, 2017